Cell Reports, Volume *27*

Supplemental Information

Development of a Cx46 Targeting Strategy for Cancer Stem Cells

Erin E. Mulkearns-Hubert, Luke A. Torre-Healy, Daniel J. Silver, Jennifer T. Eurich, Defne Bayik, Emily Serbinowski, Masahiro Hitomi, John Zhou, Bartlomiej Przychodzen, Renliang Zhang, Samuel A. Sprowls, James S. Hale, Tyler J. Alban, Artem Berezovsky, Brent A. Bell, Paul R. Lockman, Babal K. Jha, and Justin D. Lathia

Supplemental Figure S1, related to Figure 1

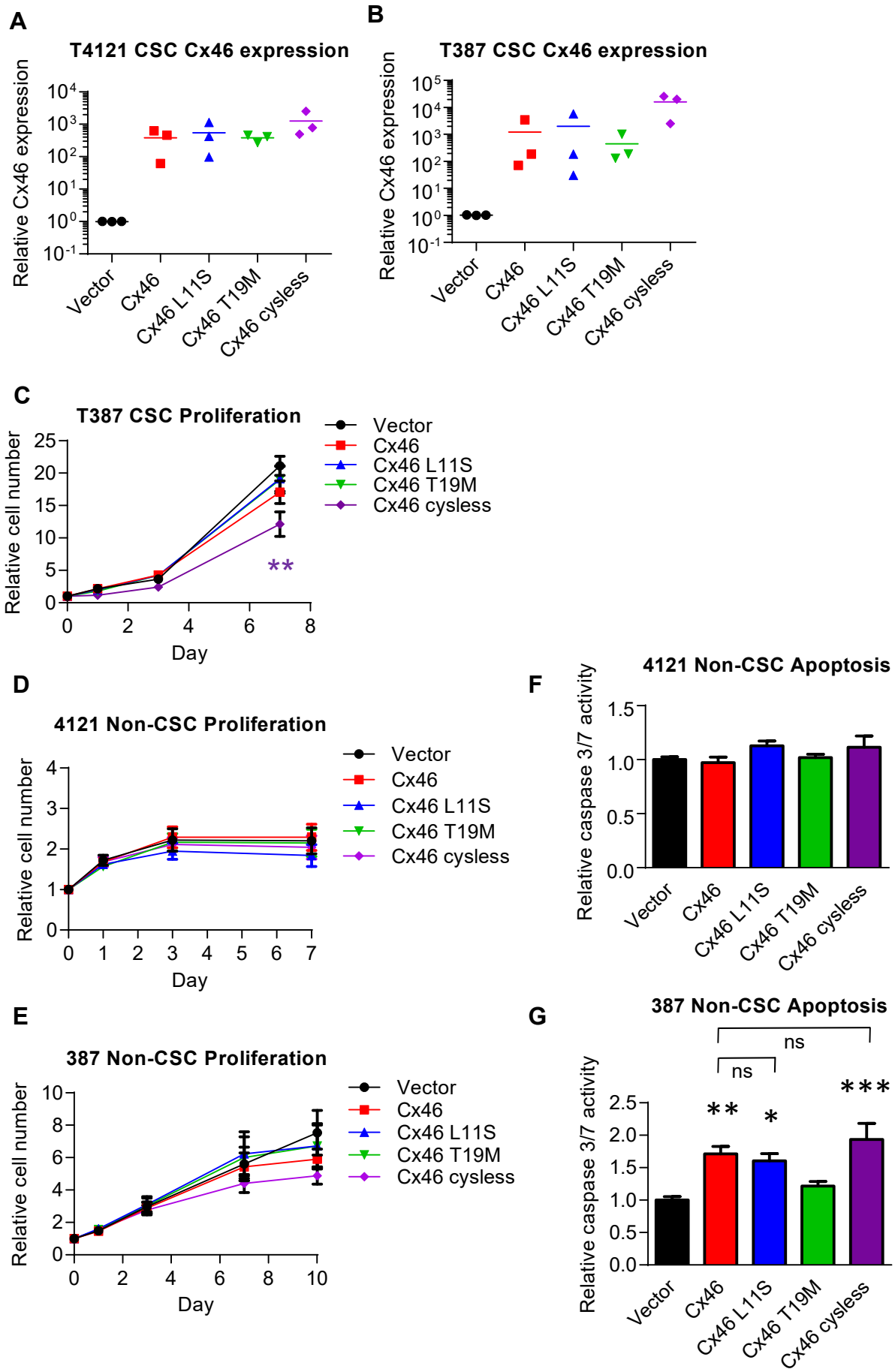

Supplemental Figure S1, related to Figure 1. Glioblastoma CSCs express Cx46 mutants. (**A-B**) CSCs from the patient-derived xenograft specimens T4121 and T387 were transfected with wildtype or mutant Cx46 and lysed for RNA 48 h later. qPCR was performed using Fast SYBR Green, and results were analyzed using the ΔΔCt method. Expression is normalized to GAPDH and is shown relative to the vector-transfected cells. n = 3 experiments performed in triplicate. All data points are shown, with the mean indicated by a horizontal line. (**C**) CSCs from the patient-derived xenograft specimen T387 were transfected with wildtype or mutant Cx46, and the number of cells was measured using CellTiter-Glo. The values shown are relative to day 0. n = 3 experiments performed in triplicate. ** $p<0.01$ by two-way ANOVA compared to vector to test for significant differences between the curves. Data are represented as mean ± SEM. (**D-E**) Non-CSCs from the patient-derived xenograft specimens T4121 (**D**) and T387 (**E**) were transfected with wildtype or mutant Cx46, and the number of cells was measured after plating using CellTiter-Glo. The values shown are relative to day 0. n = 3 experiments all performed in triplicate. There were no significant differences as assessed by two-way ANOVA compared to vector to test for significant differences between the curves. (**F-G**) Transfected non-CSCs from the patient-derived xenograft specimens T4121 (**F**) and T387 (**G**) were assessed for active caspase 3/7 on day 1 using Caspase-Glo. The values shown are normalized to the CellTiter-Glo signal at day 1 and are given relative to vector. n = 3 experiments, all performed in triplicate. * $p<0.05$, ** $p<0.01$, *** $p<0.001$ by one-way ANOVA with Bonferroni's multiple comparisons test compared to vector; a comparison to Cx46 is also shown where specified in (G).

Supplemental Figure S2, related to Figure 2

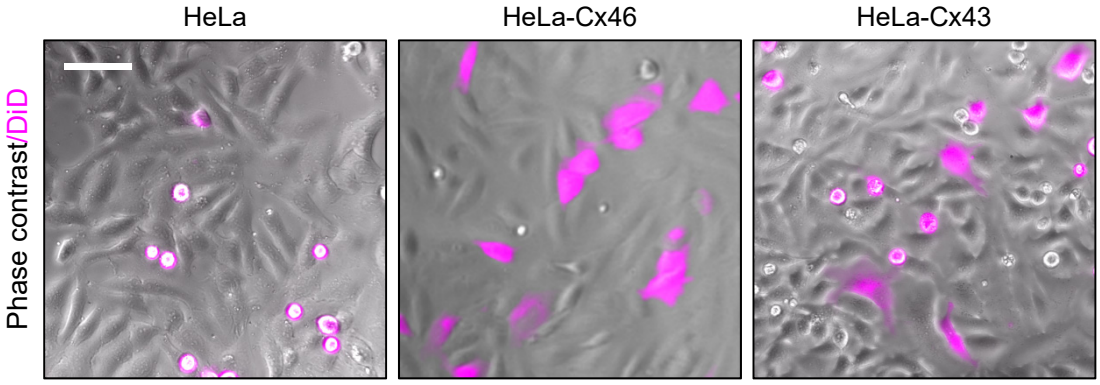

Supplemental Figure S2, related to Figure 2. Overlay of membrane fluorescence on phase contrast of the images shown in Fig. 2B. The phase contrast image of the monolayer corresponding to the images in Fig. 2B are shown with the DiD membrane fluorescence overlaid.

Supplemental Figure S3, related to Figure 4

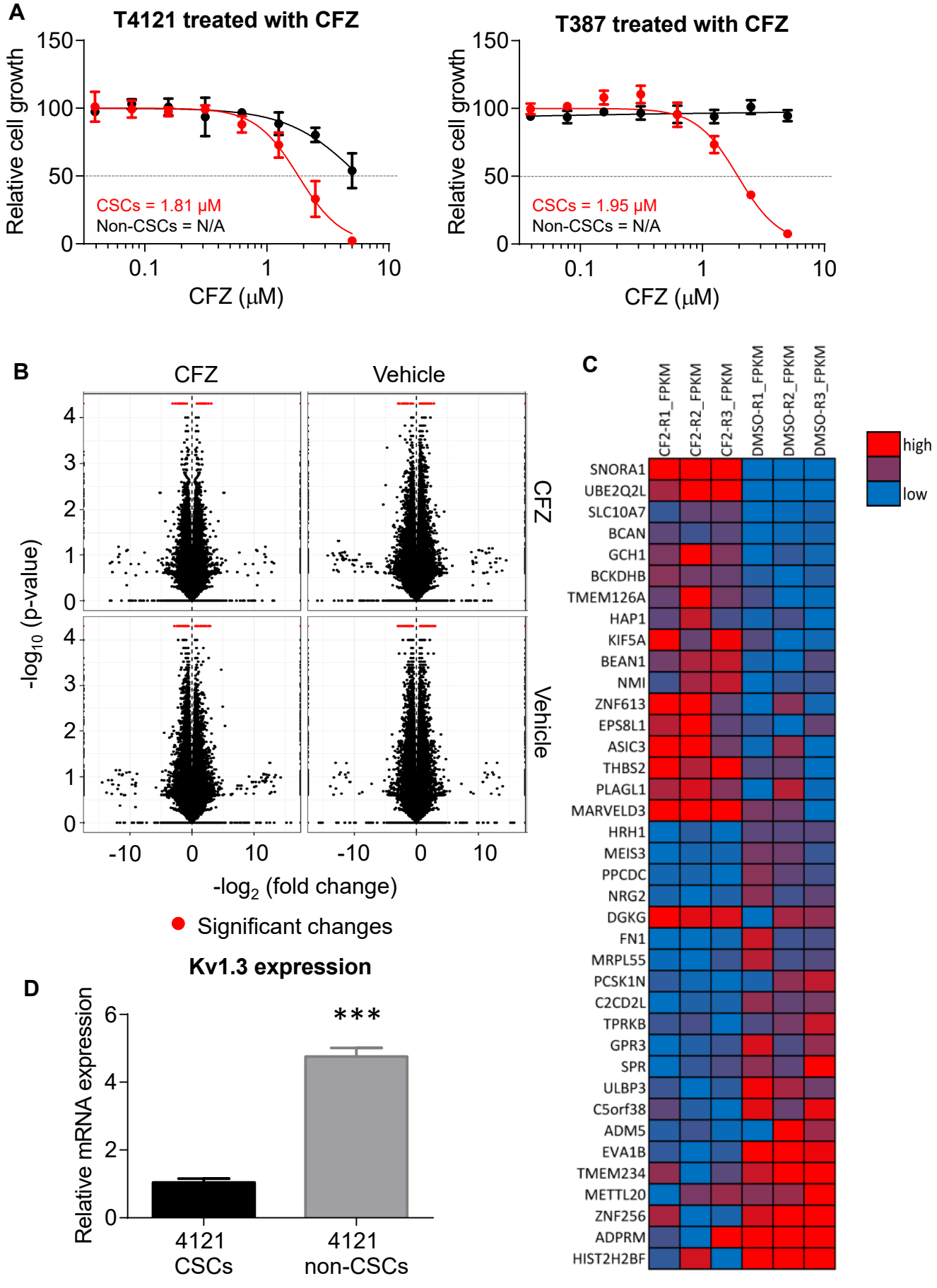

Supplemental Figure S3, related to Figure 4. Clofazimine likely acts specifically to inhibit Cx46-mediated GJIC in CSCs. (**A**) Example IC_{50} curves for clofazimine (CFZ) in two GBM specimens. Cells were treated with increasing concentrations of clofazimine for 72 h, and cell number was determined using CellTiter-Glo. The dotted gray lines indicate 50% growth inhibition. (**B**) T4121 CSCs were treated with 2 μM clofazimine for 6 hours and subjected to RNA sequencing in triplicate. Volcano plots show the distribution of changes in transcripts by RNA sequencing. Genes with significant changes are shown as red dots. (**C**) Heatmap showing the RNA sequencing hits with the largest changes with clofazimine treatment compared to DMSO vehicle. Red indicates higher expression, while blue indicates lower expression within each gene. (**D**) T4121 CSCs and non-CSCs were lysed for RNA and subjected to qPCR for Kv1.3. n = 3 experiments, with three technical replicates each. * $p<0.05$ by unpaired Student's t-test with Welch's correction compared to expression in CSCs. Data are represented as mean ± SEM.

Supplemental Figure S4, related to Figure 5

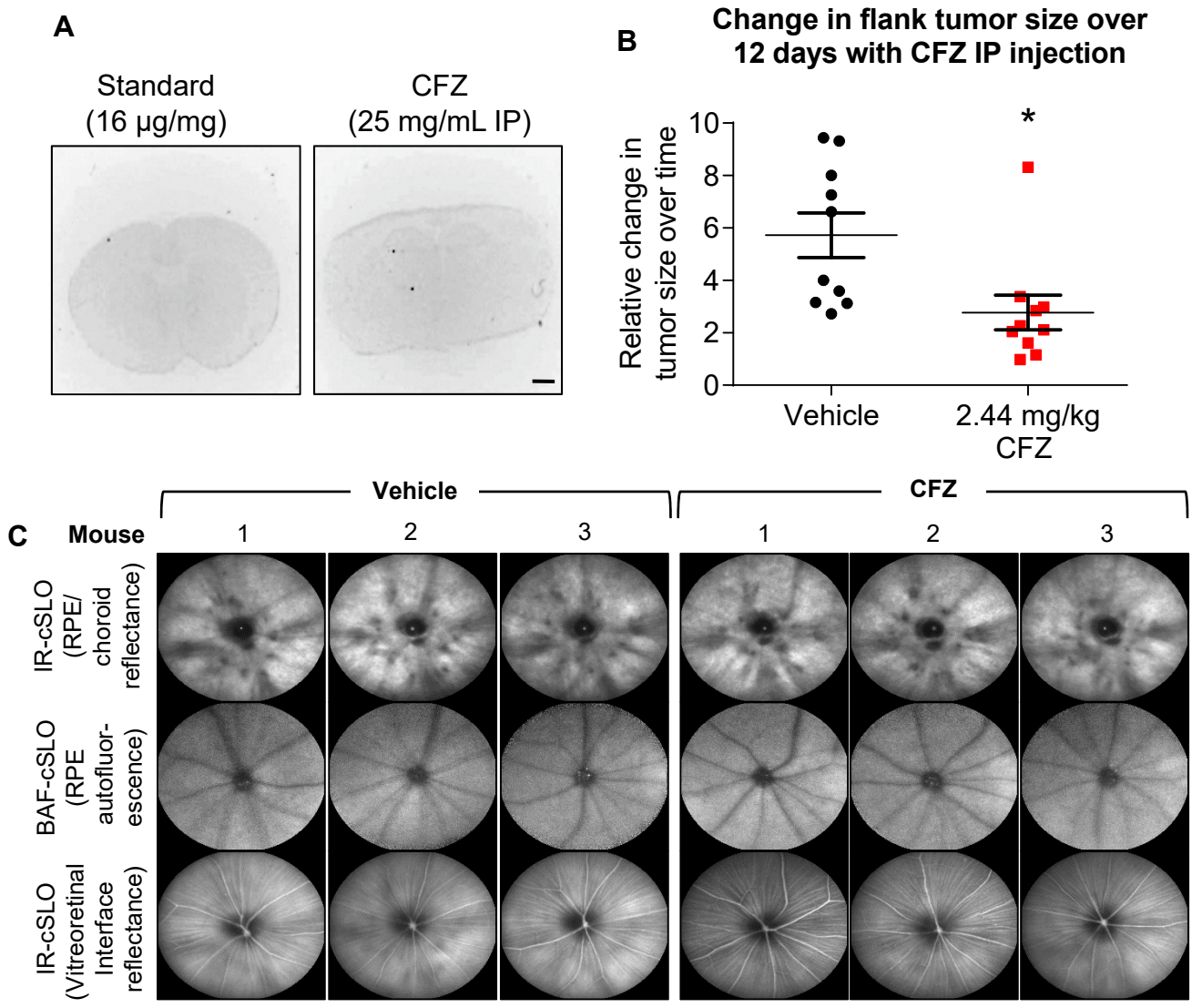

Supplemental Figure S4, related to Figure 5. Clofazimine does not cross the blood-brain barrier. (**A**) Brain sections of mice treated with clofazimine. Animals were treated IP with 25 mg/ml clofazimine or vehicle (not shown), and the drug was allowed to circulate for 10 minutes. The innate red fluorescence of clofazimine in the treated brain is compared to a brain incubated with the lowest concentration of clofazimine standard (16 μg/mL). Images are inverted to show fluorescence as black puncta. Bar, 1 mm. (**B**) Female NSG mice (n = 4 per arm) were injected with $1x10^6$ T4121 CSCs into their right flanks. Three weeks later, when tumors became palpable, animals were treated with 2.44 mg/kg clofazimine in 100 μL corn oil by IP injection. Tumor size was measured using digital calipers, and the change in tumor volume over time is provided. * $p<0.05$ by Student's t-test with Welch's correction. The data are shown as the mean and SEM, and all data points are shown. n = 10 mice per arm. (**C**) Representative confocal scanning laser ophthalmoscope (cSLO) images from the retinas of three control and three clofazimine-treated mice. The central black disk is the optic nerve. Image FOV diameter = ~1.6 mm. Infrared (IR)-cSLO images show IR signal at a wavelength of 800 nm being reflected from immediately adjacent retinal pigment epithelial (RPE) cells and choroidal tissue structures. Blue-light fundus autofluorescence (BAF)-cSLO images show the autofluorescence (excitation 488 nm/emission 500-700 nm) spanning signal emerging from the RPE monolayer that is specific to age-related lipofuscin accumulation from daily photoreceptor outer segment phagocytosis. IR-cSLO images of the vitreoretinal interface show the superficial retinal vasculature and nerve fibers originating from the optic nerve. Any toxicity to the retina of clofazimine treatment would have elicited strong inflammatory responses at one or more of the locations that would have been easily observed by non-invasive cSLO imaging.

Supplemental Table S1, related to Figure 1.

Mutant	Reported effect on Cx46 function			Our observed phenotype in CSCs		
	Hemi-channel	**Channel**	**System**	**Growth**	**Survival**	**Self-renewal**
L11S	↓	↓	Xenopus oocytes (Tong et al. Am J Physiol Cell Physiol 2013)	↓	—	—
T19M	↑	—	Xenopus oocytes and HeLa cells (Tong et al. J Membrane Biol 2015)	—	—	—
Cysless	—	↓↓↓	Granulosa and MDCK cells (Tong et al. J Cell Sci.2007)	↓↓↓	↓↓↓	↓↓↓

Supplemental Table S1, related to Figure 1. Summary table showing the published effects of each mutant on GJ and hemichannel activity when co-expressed with wild-type Cx46 and our observed effects on CSC characteristics. "–" indicates no change was observed.

Supplemental Table S2, related to STAR Methods.

Primer Name	Sequence (5’ – 3’)
Cx46 L11S F	AGCTTTCTGGGAAGACTCTCAGAAAATGCACAGGAGCAC
Cx46 L11S R	GTGCTCCTGTGCATTTTCTGAGAGTCTTCCCAGAAAGCT
Cx46 T19M F	AATGCACAGGAGCACTCCATGGTCATCGGCAAGGTTTGG
Cx46 T19M R	CCAAACCTTGCCGATGACCATGGAGTGCTCCTGTGCATT
Cx46 C54A F	GAGCAGTCAGACTTCACCGCCAACACCCAGCAGCCGGGC
Cx46 C54A R	GCCCGGCTGCTGGGTGTTGGCGGTGAAGTCTGACTGCTC
Cx46 C61A F	AACACCCAGCAGCCGGGCGCCGAGAACGTCTGCTACGAC
Cx46 C61A R	GTCGTAGCAGACGTTCTCGGCGCCCGGCTGCTGGGTGTT
Cx46 C65A F	CCGGGCGCCGAGAACGTCGCCTACGACAGGGCCTTCCCC
Cx46 C65A R	GGGGAAGGCCCTGTCGTAGGCGACGTTCTCGGCGCCCGG
Cx46 C181A F	CTGAAGCCGCTCTACCGCGCCGACCGCTGGCCCTGCCCC
Cx46 C181A R	GGGGCAGGGCCAGCGGTCGGCGCGGTAGAGCGGCTTCAG
Cx46 C186A F	CGCGCCGACCGCTGGCCCGCCCCCAACACGGTGGACGCC
Cx46 C186A R	GGCGTCCACCGTGTTGGGGGCGGGCCAGCGGTCGGCGCG
Cx46 C192A F	GCCCCCAACACGGTGGACGCCTTCATCTCCAGGCCCACG
Cx46 C192A R	CGTGGGCCTGGAGATGAAGGCGTCCACCGTGTTGGGGGC

Supplemental Table S2, related to STAR Methods. Cx46 cloning primer sequences used.